

# Network Activity and Ethereum Gas Prices

Dimitrios Koutmos

Department of Accounting, Finance, and Business Law, College of Business, Texas A&M University—Corpus Christi, Corpus Christi, TX 78412, USA; dimitrios.koutmos@tamucc.edu; Tel.: +1-361-825-5700

**Abstract:** This article explores the extent to which network activity can explain changes in Ethereum transaction fees. Such fees are referred to as “gas prices” within the Ethereum blockchain, and are important inputs not only for executing transactions, but also for the deployment of smart contracts within the network. Using a bootstrapped quantile regression model, it can be shown that network activity, such as the sizes of blocks or the number of transactions and contracts, can have a heterogeneous relationship with gas prices across periods of low and high gas price changes. Of all the network activity variables examined herein, the number of intraday transactions within Ethereum’s blockchain is most consistent in explaining gas fees across the full distribution of gas fee changes. From a statistical perspective, the bootstrapped quantile regression approach demonstrates that linear modeling techniques may yield but a partial view of the rich dynamics found in the full range of gas price changes’ conditional distribution. This is an important finding given that Ethereum’s blockchain has undergone fundamental economic and technological regime changes, such as the recent implementation of the Ethereum Improvement Proposal (EIP) 1559, which aims to provide an algorithmic updating rule to estimate Ethereum’s “base fee”.

**Keywords:** blockchain; DeFi; Ethereum; gas price; London hard fork (EIP-1559)

## 1. Introduction

The advent of blockchain technology has given rise to a flourishing ecosystem of decentralized systems, tools, and communities (Bowden et al. 2021; Faqir-Rhazoui et al. 2021; King et al. 2021; Vacca et al. 2021; Zheng et al. 2023). Apart from the ever-growing number of cryptocurrencies and crypto-based exchanges, this has also catalyzed a flurry of innovations in financial engineering, such as cryptocurrency derivatives and their associated exchanges, asset-based cryptocurrencies, financialization schemes for dispute resolution platforms (i.e., “cryptocourts”), and a range of other crowdsourcing-type methods for raising funds or assembling teams and knowhow to find solutions to problems (Cai 2018; Dylag and Smith 2023; Lipton 2018; Risius et al. 2023).

Generally speaking, the three key features and properties of blockchain are as follows: (i) openness and transparency in terms of either transaction or operational activity, or data flowing within, say, a supply chain network (Gligor et al. 2022); (ii) a certain immutability element built in to the network which is designed to protect the history of data and prevent bad actors from altering it for either nefarious or self-serving purposes (Faqir-Rhazoui et al. 2021); (iii) a certain inherent security, given that blockchains are based upon decentralized frameworks, such as consensus and cryptographic hash functions (Fernandez-Carames and Fraga-Lamas 2020).

Altogether, these three properties have sparked much interest in the design and application of cryptocurrencies (Yuan and Wang 2018), the possible use cases of blockchain in supply chain and health care networks (Hölbl et al. 2018; Saberi et al. 2019), and in the broader integration of blockchain into various facets of our everyday life (Kshetri and Voas 2018; Ochôa et al. 2021). Bitcoin is arguably the very first wide-spread application of blockchain technology (Nakamoto 2008). In terms of transaction usage, trade volume, mar-



**Citation:** Koutmos, Dimitrios. 2023. Network Activity and Ethereum Gas Prices. *Journal of Risk and Financial Management* 16: 431. <https://doi.org/10.3390/jrfm16100431>

Academic Editor: Shigeyuki Hamori

Received: 21 August 2023

Revised: 17 September 2023

Accepted: 18 September 2023

Published: 30 September 2023



**Copyright:** © 2023 by the author. Licensee MDPI, Basel, Switzerland. This article is an open access article distributed under the terms and conditions of the Creative Commons Attribution (CC BY) license (<https://creativecommons.org/licenses/by/4.0/>).

ket capitalization, and the overall attention it receives, bitcoin has remained the dominant cryptocurrency (Koutmos and Wei 2023; Marzo et al. 2022).

Ethereum is currently the second largest cryptocurrency in terms of market capitalization, despite its launch in July 2015—approximately six years after the launch of bitcoin (Buterin 2014). Its popularity has particularly grown in recent years given that the Ethereum infrastructure not only circulates its own native cryptocurrency (Ether) that users can transact with, but also enables the development of a range of decentralized applications (dApps) and smart contracts. This is enabled through the so-called “Ethereum Virtual Machine” (EVM). The EVM is a quasi-Turing complete 256-bit “computer,” in which all transaction or smart contract activity is stored locally on each node of the network (Dannen 2017). The EVM is a virtual machine consisting of a network of computers and is accessible globally by anyone who has a node (i.e., wallet application). The EVM is quasi-Turing complete in the sense that sets of inputs or instructions (such as those embedded within a smart contract) can be executed on the Ethereum blockchain. However, such executions depend on, and are fundamentally limited to, the quantity of and users’ willingness to pay for “gas”. Gas serves as the transaction fee and is a critical component of the Ethereum ecosystem. By having to pay for, say, the development and execution of smart contracts, this theoretically maximizes the likelihood that users will construct bona fide smart contracts to satisfy their unique needs and preferences, rather than develop needless contracts with never-ending programs that are resource- and energy-intensive.

Gas prices thus constitute a fundamental element within the Ethereum ecosystem. This article further discusses this and builds and estimates a bootstrapped quantile regression model to quantify the relation between network activity and gas prices across the conditional distribution of gas price changes. Using this bootstrapped quantile regression approach, which accounts for heteroskedasticity and ensures robustness in results, this article shows reliable evidence that network activity is linked to changes in gas prices. Such a linkage, however, can vary across regime periods and from periods of extreme negative price changes (lower conditional quantiles) to periods of extreme positive price changes (higher conditional quantiles). Finally, this bootstrapped quantile regression approach is advantageous given the recent implementation of Ethereum Improvement Proposal (EIP) 1559 (EIP-1559), which aims to provide an algorithmic updating rule to estimate Ethereum’s “base fee”. As is discussed in more detail, this proposal aimed to reduce variability and unpredictability in the fluctuations of Ethereum gas prices.

The remainder of this article is structured as follows. Section 2 contains a conceptual discussion on Ethereum gas prices and how they are used as a transaction fee within the Ethereum ecosystem. It also discusses EIP-1559 and what it means for the Ethereum community, as well as implications for the time series behavior of gas prices. Section 3 describes the data used in this article, along with some of their time series properties. Section 4 outlines the quantile regression approach and its implementation. Section 5 discusses the major findings. Finally, Section 6 concludes and provides avenues for future research.

## 2. “Gas” as a Transaction Fee and EIP-1559

Transaction fees are typically paid when a user initiates an action that is to be recorded on the blockchain. Such actions can range in complexity, from sending cryptocurrency to another party or using a dApp to perform more complicated actions such as borrowing and lending or executing the terms of a smart contract. Depending on the consensus mechanism of the particular blockchain, these transaction fees serve to compensate network validators, which ensure the maximization of the probability that activity within the blockchain is recorded fairly and accurately.

Prior to the implementation of EIP-1559, the Ethereum ecosystem behaved like a generalized first-price auction whereby users select and submit a gas price (bid), indicating how much they are willing to pay in order for their transaction to be processed and included in the blockchain. In such a system, miners (auctioneers) rationally allocate priority to those transactions which had the highest submitted gas price (i.e., the highest bidders). The

Ethereum network was thus susceptible to the usual problems which plague first-price auctions, such as (i) non-truthful bidding, (ii) (un-)intentional overbidding, and, given (i) and (ii), (iii) excess intra- and inter-block gas price volatility (Reijsbergen et al. 2021). Such gas price volatility can jeopardize users' confidence in the network and hinder their ability to accurately forecast or calculate appropriate fees for their transactions in real time.

The EIP-1559 reforms seek to address the market inefficiencies arising from Ethereum's first-price auction market mechanism. As is discussed further, a vital feature of EIP-1559 is the initiation of a base fee that is algorithmically adjusted by the protocol depending on the degree of demand and network congestion. In other words, the base fee fluctuates in accordance with the supply and demand for gas.

More specifically, and using the notation of Leonardos et al. (2021), EIP-1559 proposes certain key aspects for bids. First, a fee cap,  $f$ , which is a maximum fee that a user is willing to pay for their transaction to be processed and recorded on the blockchain. Second, a premium,  $p$ , which is the user's maximum tip that they are willing to pay for the miner to process their transaction and have it recorded on the blockchain. In this way, a miner will never receive more than  $p$  and a user will never pay more than  $f$ . Such an arrangement serves to minimize the probability that a given miner (validator) with more than 50% of the computational mining power will engage in dishonest strategies, such as proposing empty blocks for the purpose of increasing future base fees (Azouvi et al. 2023).

Furthermore, and in keeping with the notation of Leonardos et al. (2021), let us denote the base fee as  $b_t$ , whereby  $t > 0$ . In this case, the subscript  $t$  denotes the block height, which is measured by the quantity of blocks that have been validated since the inception of the underlying blockchain. Thus, users who perform a transaction that is validated and included in a certain block  $B_t$  need to pay the prevailing base fee,  $b_t$ , that is specific to that block. However, this base fee is then "burned" (i.e., it is permanently eliminated from the circulating money supply of Ether) instead of being used to compensate the miner. Therefore, a miner's tip can be expressed as:

$$\text{miner's tip} \triangleq \min \{f - b_t, p\} \tag{1}$$

According to EIP-1559, and with blocks that have size  $T$  (measured in gas) and with a target block load of  $T/2$ , let  $g$  represent the number of transactions that are ultimately validated and included into a certain block,  $B_t$ . Given that  $g$  is conditional on the prevailing base fee,  $b$ , we can write:

$$b_{t+1} = b_t(1 + d \cdot [(g_t|b_t - T/2)/(T/2)]) \tag{2}$$

and where  $d$  is a "learning parameter", or an "adjustment parameter", that is currently set at  $d = 0.125$ . The base fee thus adjusts dynamically with respect to the degree of congestion within the Ethereum ecosystem. For example, if  $g_t > T/2$  (i.e., more transactions than targeted are validated and included in the block), then the future base fee will rise. This rise is scaled by the adjustment parameter  $d$  and commensurate to the degree which  $g_t$  exceeds  $T/2$ . Conversely, if  $g_t < T/2$ , then the future base fee will decrease. Finally, there is an "equilibrium" in the future base when  $g_t = T/2$ , whereby the future base fee remains constant.

Conventionally, gas prices are not expressed in Ether, but rather in more granular units referred to as "wei" and "Gwei", whereby  $1 \text{ Ether} = 10^{18} \text{ wei}$  and  $1 \text{ Ether} = 10^9 \text{ Gwei}$ . Thus, there are 1 billion wei for every one Gwei. Figure 1 shows the time series evolution of Ethereum gas prices (expressed as the natural log of wei) for the sample period of this article (1 September 2015 through 26 May 2023). The vertical red line denotes the implementation of EIP-1559 that happened on 5 August 2021. The vertical green line denotes when Ethereum moved fully to proof-of-stake (PoS) from proof-of-work (PoW).

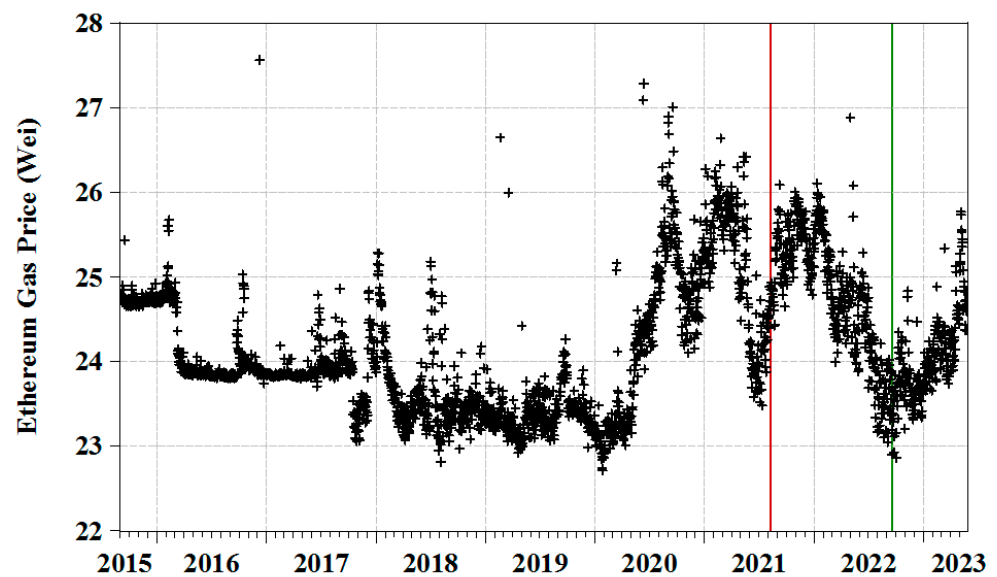


**Figure 1.** Time series plot of Ethereum gas prices. This figure shows a time series plot of Ethereum gas prices (in Wei) in their natural log levels for the entire sample period (1 September 2015 through 26 May 2023). The vertical red line denotes when the Ethereum Investment Proposal (EIP) 1559 (i.e., the so-called “London upgrade”) was implemented, which happened on 5 August 2021. The vertical green line denotes when Ethereum moved fully to proof-of-stake (PoS), which happened on 15 September 2022.

As can be seen from Figure 1, Ethereum gas prices were, relatively speaking, least volatile from September 2015 to September 2017. From the beginning of 2018 to the end of 2019, gas price volatility rose. This time period coincides with a significant bear period for Ethereum, where it had an arithmetic mean return of approximately  $-85\%$ . Afterwards, Ethereum prices rose while also becoming more volatile. In Figure 1, we can see that from the beginning of 2020 up until the end of the sample period, Ethereum gas prices experienced the most volatility. This is an important observation, especially given that the motivation for EIP-1559 is to reduce the uncertainty surrounding Ethereum gas prices in order to ensure more predictable transaction costs for all its users.

Figure 2 shows a scatter plot between Ethereum gas prices (expressed as the natural log of *wei*) and Google Search Volume (GSV), which is measured according to a normalized range (from 0 to 100) that Google Trends<sup>TM</sup> utilizes. The plot, while preliminary, shows a rather positive relation between market attention (GSV) and Ethereum gas prices. However, as the K-nearest neighbor fit line shows (in green), this relation is hardly linear in nature. In addition, most observations in the sample are accounted for when GSV is between 0 and 20.

At a minimum, Figures 1 and 2 show that Ethereum gas prices can undergo distinct and non-linear price regimes, either stemming from technical changes in Ethereum’s ecosystem (like the implementation of EIP-1559 and the move to PoS), or due to exogenous forces such as market attention. As is discussed further, the bootstrapped quantile regression approach in this article is designed to capture some of these distinct price regimes.

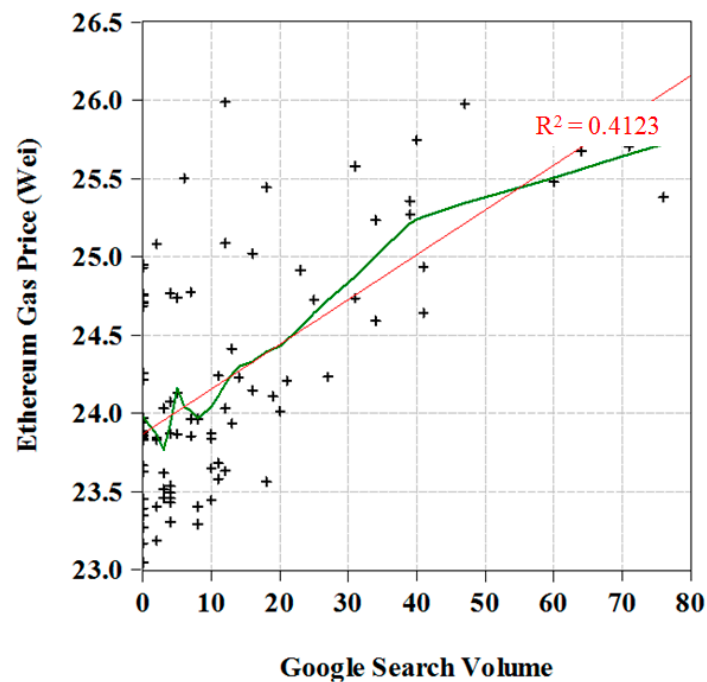


**Figure 2.** Google Trends<sup>TM</sup> and Ethereum gas prices. This figure shows a scatter plot of Ethereum gas prices (y-axis) against Google Trends<sup>TM</sup> for the entire sample period (1 September 2015 through 26 May 2023). The data in this scatter plot are in monthly frequency for illustrative purposes. Ethereum gas prices on the y-axis are in their natural log levels, while Google search volume is expressed on a normalized range of 0 to 100 (see URL: <https://support.google.com/trends/answer/4365533?hl=en>) (accessed on 20 August 2023) The red line is a slope estimate using an OLS regression, which has an  $R^2$  of 0.4123. The green line is a K-nearest neighbor fit line.

### 3. Data Description

To examine the extent to which Ethereum gas prices can be explained by fundamental aspects of Ethereum's network, this article collects daily time-series data (7 days a week) on Ethereum gas prices and a sample of network activity variables from 1 September 2015 until 26 May 2023. This comprehensive sample range encompasses a host of significant developments and trends, such as the introduction of futures markets for Bitcoin (in December of 2017), certain countries' wide-spread adoption of cryptocurrencies (such as El Salvador), the growing interest in financially and technologically engineered offshoot crypto investment vehicles (such as non-fungible tokens and crypto ETFs), high-profile individuals' (and celebrities') contributions to cryptocurrency attention in the media and press, the emergence of cryptocurrency lobbyists, and the conceptual development of so-called central bank digital currencies (CBDCs), to name but a few examples. During this sample range, and as mentioned, Ethereum underwent its own unique developments, such as the implementation of EIP-1559 and its move from PoW to PoS.

Apart from Ethereum gas prices, and for the sample period 1 September 2015 until 26 May 2023, this article collects data on the following network activity features of Ethereum's blockchain:<sup>1</sup>

- (i) *Ethereum Prices (ETH Price)*: Data on Ethereum's market prices (in USD) are gathered as a proxy for investors' expectations for the overall market value of Ethereum. Rising cryptocurrency prices can be associated with rising user and investor sentiment, while declining prices can signal market fragility, users' anticipation of losses, or imminent strategic attack by miners and validators (Sockin and Xiong 2023).
- (ii) *Number of Intraday Transactions (Transactions)*: Data on the number of intraday transactions on the Ethereum blockchain are gathered as a proxy for fundamental value for Ethereum. While cryptocurrencies are alluring for a number of reasons, one of their

primary uses are a quick and transparent means of payment among users. In network theory, whether we are attempting to value a social media platform (such as Twitter, Facebook, or LinkedIn), an online customer-to-customer (C2C) entity (such as Ebay), a business-to-business (B2B) entity (such as Amazon, Slack, or Alibaba), or a landline telecom company (such as, say, a portion of AT&T's business model), the number of users (and usage activity) is a variable that is of fundamental importance. For example, some of the early literature on cryptocurrencies attempts to use Metcalfe's Law to determine the value of, say, Bitcoin, and the extent to which deviations from such laws can be interpreted as price bubbles (Wheatley et al. 2019).

- (iii) *Number of Ethereum Requests for Comment (ERC20)*: Data on the number of intraday ERC20 tokens that are transferred are gathered to proxy for smart contract and smart property activity. As mentioned, Ethereum enables the development and execution of dApps. Such dApps can involve the acceptance or transfer of Ether or some alternate (off-blockchain) asset or agreement. As Rahimian et al. (2019) discuss, the need has arisen for interoperable tokens that can interact with other dApps, WebApps, and other such exchange services that facilitate the trading of tokens. Further to this purpose, Ethereum accepted the proposed standard called ERC20, which defines technical standards for actions and rules that, say, tokens or smart contracts must contain in order to be implementable.
- (iv) *Ethereum Average Block Size (Block Size)*: Data on the daily average block size (in bytes) are gathered to proxy for network validation activity. As shown in Equation (2), block size can serve as a proxy for the degree of congestion (demand) within the Ethereum blockchain. While Ethereum currently has a target block size, on any given day, and given the degree of congestion within the network, block sizes are variable. As discussed, and as part of EIP-1559, if the current actual block size exceeds the target size, the Ethereum protocol will increase the base fee for the upcoming block. Conversely, if the current actual block size is below the target size, the base fee for the upcoming block will decrease. Such a dynamically adjustable base fee, that is conditional on network congestion (user demand for validators), is designed to support a long-run equilibrium for Ethereum's block size. This process is known as "tâtonnement", a notion originally conceived by Léon Walras, a French economist and mathematician. Tâtonnement refers to the derivation of a "solution" to a mathematical iterative sequence in order to achieve some equilibrium (Walker 1988). Translated directly from French, tâtonnement means "trial and error." In terms of the Ethereum ecosystem, if  $g_t \neq T/2$  (error), then there is a commensurate change to the upcoming block's base fee (trial). This process (re-)iterates in order to support an equilibrium in the long-run evolution of block size.
- (v) *Ethereum Average Block Time (Block Time)*: Data on the daily average block time (in seconds) are gathered to proxy for network validation activity. This reflects the time taken for a block to be validated and included into the Ethereum blockchain. While still in its initial stages, a budding area of research is exploring the benefits of EIP-1559 on the overall Ethereum network and user experience. Liu et al. (2022) argue that the implementation of EIP-1559 improved the user experience, enhanced predictability in gas prices, and reduced waiting times for transactions.
- (vi) *Ethereum Verified Contracts (Contracts)*: Data on the total number of intraday verified smart contracts are gathered to proxy for network demand and contract activity on the Ethereum blockchain. At any given time, verified contracts are viewable (along with, for example, the address, contract name, compiler for the contract, and Ether balance).<sup>2</sup> Looking at the number of smart contracts in addition to, say, the number of Ethereum transactions can provide potentially meaningful and unique information, especially since only a fraction of the total number of smart contracts can be associated with the highest volume of transactions on the Ethereum blockchain (Oliva et al. 2020).

Table 1 provides distributional statistics for each of the aforementioned variables. Panels A and B show these statistics when the variables are in their natural logarithmic

levels, as well as their natural logarithmic first-differences (in %), respectively. When specifically looking at Panel B, we can see that many of these variables exhibit a high degree of volatility, and their time-series behaviors do not conform to what is theoretically observed in a normal distribution. This is a stylized fact in financial time-series data and is especially so when working with cryptocurrency data. For example, and when looking at Ethereum price changes, we can see that during extreme bear periods (i.e., the 10th percentile), Ethereum can arithmetically lose about a quarter of its value within a day. Likewise, and during a strong bull period (i.e., the 90th percentile), Ethereum investors can gain this amount within a day.

**Table 1.** Distributional characteristics of the data.

	p10	p25	p50	p75	p90	p99	Mean	Std. Dev.	Skew.	Kurt.
Panel A: Log levels in data series										
<i>Eth Gas Price</i>	23.2622	23.5180	23.9084	24.7086	25.3547	26.0965	24.1534	0.7861	0.7768	2.9992
<i>Eth Price</i>	2.3085	4.8385	5.6869	7.2567	7.8780	8.3659	5.9150	1.6621	−0.6640	2.8475
<i>Transactions</i>	10.5755	12.5800	13.5047	13.9191	14.0142	14.1868	13.2387	1.0453	−1.6330	4.3962
<i>ERC20</i>	6.8077	11.6535	12.9842	13.5328	13.7273	13.9155	12.2538	2.1379	−1.8420	5.1290
<i>Block Size</i>	7.2861	9.3370	10.0799	10.9228	11.3674	11.6640	10.0767	1.2185	−1.0484	3.3593
<i>Block Time</i>	2.5610	2.5756	2.6093	2.6686	2.8231	3.1976	2.6337	0.1313	3.1125	15.5820
<i>Contracts</i>	1.6094	3.8501	4.6298	5.5568	6.2162	6.7117	4.3917	1.6361	−1.0509	3.5952
Panel B: Log first-differences in data series (in %)										
<i>Eth Gas Price</i>	−22.5586	−8.7377	−0.1380	7.6927	23.1492	79.3890	−0.0204	29.5126	0.0338	45.5546
<i>Eth Price</i>	−5.6127	−2.2890	0.0270	2.8965	6.4481	16.6153	0.2531	5.8227	−0.2876	10.2711
<i>Transactions</i>	−9.8942	−4.4681	−0.0540	4.5377	10.5995	29.4438	0.2517	9.5925	0.3941	12.2167
<i>ERC20</i>	−23.5492	−7.9911	0.0000	7.4382	22.0067	163.1082	0.7846	41.9667	2.2599	45.7036
<i>Block Size</i>	−9.3970	−4.0776	−0.0646	4.3151	9.7661	27.3541	0.2530	9.3279	0.8488	20.7955
<i>Block Time</i>	−1.6504	−0.7282	0.0000	0.8158	1.6654	4.5901	−0.0142	2.1670	−5.9685	113.7394
<i>Contracts</i>	−45.4199	−18.8518	0.0000	17.9393	46.8110	138.6294	0.0811	46.5757	0.1534	8.7750

This table reports distributional statistics for the natural log levels of each of our variables (in Panel A) and the natural log first-differences in our variables (in Panel B); specifically, the 10th, 25th, 50th, 75th, 90th, and 95th percentiles, respectively, as well as the mean, standard deviation, skewness, and kurtosis. Section 3 of the article discusses these data series and their properties further. The entire sample period for this analysis is from 1 September 2015 through 26 May 2023 and the frequency of the data is daily (and includes weekend data).

Stationarity tests are also conducted and shown in Table 2. Panels A and B show these statistics when the variables are in their natural logarithmic levels, as well as their natural logarithmic first-differences (in %), respectively. For each of the variable series, the augmented Dickey–Fuller (ADF) test (Dickey and Fuller 1981), the Phillips–Perron (PP) test (Phillips and Perron 1988), and the Kwiatkowski–Phillips–Schmidt–Shin (KPSS) test (Kwiatkowski et al. 1992), respectively, are shown. The purpose of these three unit root tests is to provide confirmatory evidence that all the variables in their natural logarithmic first-difference form (in Panel B) do not contain a unit root (i.e., are stationary), so we can then move to performing our bootstrapped quantile regression model. Taking just the natural logarithm of the variables in their level form (in Panel A) does not necessarily induce stationarity, as all the three tests confirm. Generally speaking, regression models using non-stationary variables can yield spurious results.

Table 2. Unit root tests.

Data Series	ADF	PP	KPSS	ADF	PP	KPSS
	Panel A: Log Levels in Data Series			Panel B: Log First-Differences in Data Series (in %)		
Eth Gas Price	−0.0816	−0.2069	0.5729 *	−12.6670 *	−84.1643 *	0.0116
Eth Price	0.7745	1.2006	0.6099 *	−9.8349 *	−55.1253 *	0.1020
Transactions	2.3065	2.1105	1.2707 *	−11.0760 *	−98.1462 *	0.0723
ERC20	1.2433	0.3942	1.3546 *	−12.0559 *	−117.2685 *	0.0555
Block Size	2.5882	1.6090	0.9475 *	−12.6599 *	−83.1809 *	0.0281
Block Time	−0.6539	−0.7685	1.3430 *	−32.3120 *	−55.2876 *	0.0199
Contracts	1.6436	−0.8438	0.6329 *	−13.0969 *	−136.5858 *	0.0082

This table reports unit root test statistics for the natural log-levels and natural log-changes, respectively, for each of the data series used for the entire sample period (1 September 2015 through 26 May 2023). The frequency of the data is daily (and includes weekend data). The unit root tests applied are the augmented Dickey–Fuller (ADF), Phillips–Perron (PP), and Kwiatkowski–Phillips–Schmidt–Shin (KPSS) test, respectively. The asterisk (\*) denotes whether the null hypothesis ( $H_0$ ) is rejected at the 1% level of significance, at least. The null hypothesis,  $H_0$ , for the ADF and PP test is that a given data series contains a unit root. Conversely, the null hypothesis,  $H_0$ , for the KPSS test is that a given data series is stationary. Optimal lag lengths for the ADF test are based on the Akaike information criterion (AIC). The PP and KPSS tests utilize the Newey–West bandwidth selection method and the Bartlett kernel spectral estimator.

#### 4. Analytical Framework

This article seeks to examine the extent to which Ethereum gas prices can be explained using the network activity variables discussed in Section 3. Given that the Ethereum ecosystem has undergone critical technological and economic regime changes, such as the implementation of EIP-1559 and its move from PoW to PoS, it is reasonable to expect distinct relations between network activity and gas prices across various sample ranges. In addition, and as shown in the quantile–quantile (Q–Q) plot in Figure 3, changes in Ethereum gas prices can deviate from a theoretically normal distribution. This observation is consistent with Table 1, which shows that the distribution of Ethereum gas prices exhibits a high degree of kurtosis, and thus thick tails.

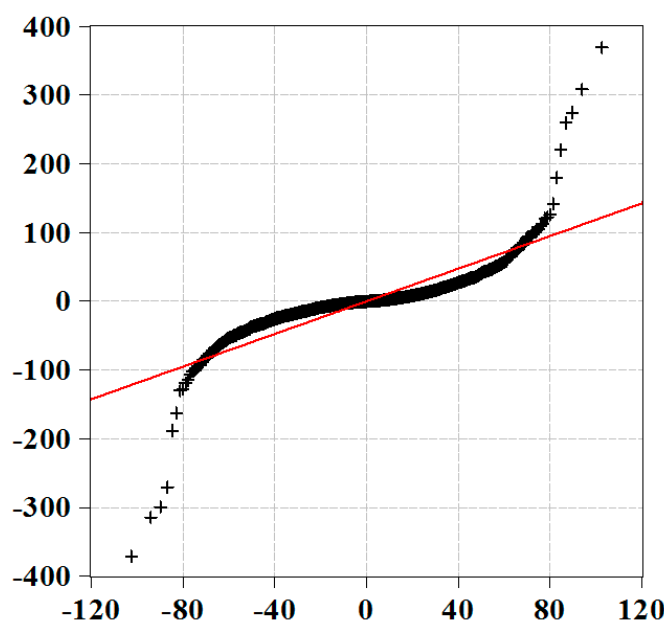


Figure 3. Quantile–quantile plot of Ethereum gas price changes. This figure shows a quantile–quantile (Q–Q) plot for Ethereum gas price changes (in percentages) for the entire sample period (1 September 2015 through 26 May 2023). The horizontal axis (x-axis) denotes the quantiles that are theoretically observable in a normal distribution. The vertical axis (y-axis) denotes the quantiles of Ethereum gas price changes.

Given that gas prices are a fundamental attribute within the Ethereum ecosystem, it is important to map the linkages between network activity and gas prices across the full distribution of gas price changes, whereby lower conditional quantiles are associated with large negative price changes and higher conditional quantiles are associated with large positive price changes. Relatively small price changes of either sign will be somewhere in the middle of the distribution. Thus, and to ensure robustness in the results, this article builds and estimates a bootstrapped quantile regression model that can accommodate the non-Gaussian nature of gas price changes, as well as being able to uncover the heterogeneous linkages between network activity variables and gas price changes. Following [Koenker and Bassett \(1978\)](#) and [Buchinsky \(1994, 1995\)](#), we can express the conditional quantile model as follows:

$$y_i = x_i' \beta_\theta + u_{\theta i} \text{ with } \text{Quant}_\theta(y_i|x_i) = x_i' \beta_\theta, \quad i = 1, \dots, n, \tag{3}$$

where  $\beta_\theta$  and  $x_i$  are  $K \times 1$  vectors and  $x_{i1} \equiv 1$ . The  $\theta$ th quantile of  $y$  given  $x$  is represented as  $\text{Quant}_\theta(y|x)$ . It is assumed that the error term,  $u_\theta \equiv y - x' \beta_\theta$  is a continuously differentiable cumulative distribution function,  $F_{u_\theta}(\cdot|x)$ , and density function  $f_{u_\theta}(\cdot|x)$ . From this assumption, it follows that  $\text{Quant}(u_\theta|x) = 0$  and  $f_{u_\theta}(0|x) > 0$ . Thus, an estimator for  $\beta_\theta$  is obtainable as:

$$\min_{\beta} \frac{1}{n} \sum_{i=1}^n \rho_\theta(y_i - x_i' \beta) \tag{4}$$

The check function can be represented as  $\rho_\theta(\lambda) = (\theta - I(\lambda < 0))\lambda$ , where  $I(A)$  is the indicator function. As shown in [Koenker and Bassett \(1978\)](#), Equation (4) is a linear programming problem.

[Powell \(1986\)](#) demonstrates that Equation (4) can methodologically fit into the generalized method of moments (GMM) model for censored quantile regression models. Furthermore, and under certain conditions ([Huber 1967](#)), it can be shown that

$$\sqrt{N}(\hat{\beta}_\theta - \beta_\theta) \xrightarrow{L} \mathcal{N}(0, \Lambda_\theta) \tag{5}$$

where

$$\Lambda_\theta = \theta(1 - \theta) (E[F_{u_\theta}(0|x)xx'])^{-1} E[xx'] (E[F_{u_\theta}(0|x)xx'])^{-1}. \tag{6}$$

For illustration, if the density of  $u_\theta$  at 0 is independent of  $x$  (i.e.,  $F_{u_\theta}(0|x) = F_{u_\theta}(0)$ ), then  $\Lambda_\theta$  can be simplified and expressed as:

$$\Lambda_\theta = \left( \theta(1 - \theta) / F_{u_\theta}^2(0) \right) (E[xx'])^{-1} = \sigma_\theta^2 (E[xx'])^{-1} \tag{7}$$

and where

$$\sigma_\theta^2 = \left( \theta(1 - \theta) / F_{u_\theta}^2(0) \right). \tag{8}$$

This article extracted estimates and standard errors through an  $(x, y)$ -bootstrapping procedure ([Buchinsky 1994, 1995](#); [Pedersen 2015](#)). This approach is conducted by drawing  $B$  sub-samples of  $(x_t, y_t)$  pairs of size  $m$  and with replacement from the  $N - 1$  pairs of the original sample pool. As discussed in [Buchinsky \(1994, 1995\)](#) and [Pedersen \(2015\)](#), among others, this approach can improve robustness in results because, first, it can accommodate the heteroskedastic nature of the time series, and second, it does not require that error terms be identically distributed. As discussed in [Figure 1](#), Ethereum gas price changes are heteroskedastic in nature and can exhibit regime shifts in their behaviors at various points in time.

Therefore, and when  $f_{u_\theta}(0|x) \neq f_{u_\theta}(0)$ , the  $(x, y)$ -bootstrapping method is utilized where, for each of the  $B$  sub-samples, an estimator for  $\hat{\beta}_\theta$  is calculated to capture  $B$  bootstrap estimates,  $\hat{\beta}_\theta^1, \dots, \hat{\beta}_\theta^B$ . As such, the estimate for  $\Lambda_\theta$  can be expressed in the following way:

$$\hat{\Lambda}_\theta = N(m/N)(1/B) \sum_{b=1}^B (\hat{\beta}_\theta^b - \hat{\beta}_\theta)(\hat{\beta}_\theta^b - \hat{\beta}_\theta)'. \tag{9}$$

After conducting extensive Monte Carlo simulations, Buchinsky (1995) illustrates that such a  $(x, y)$ -bootstrapping approach can improve robustness in coefficient estimates. For that reason, and consistent with the findings of Pedersen (2015), the size of the bootstrap samples used in this article will be equivalent to the original sample size.

### 5. Discussion of Findings

Table 3 presents the coefficient estimates for our bootstrapped quantile regression model, whereby logarithmic first-differences (in %) in Ethereum gas prices is our response variable and the network activity variables discussed in Section 3 are our predictor variables (*Eth Price*, *Transactions*, *ERC20*, *Block Size*, *Block Time*, and *Contracts*, respectively). As discussed in Section 3, all these predictor variables are in their logarithmic first-differenced (in %) form in order to induce stationarity and reduce the possibility of spurious regression results. Table 3 thus shows regression estimates across the 5th, 10th, 20th, 30th, 40th, 50th, 60th, 70th, 80th, 90th, and 95th conditional quantiles, respectively, in order to map the extent to which our network activity predictor variables can explain Ethereum gas prices across the full distribution of gas price changes. For the sake of comparison, OLS regression estimates are also shown in Table 3.

**Table 3.** Bootstrapped quantile regression estimates.

	OLS	Left Tail			Center of Distribution				Right Tail			
		0.05	0.10	0.20	0.30	0.40	0.50	0.60	0.70	0.80	0.90	0.95
<i>Eth Price</i>	-0.3755 ** (-2.756)	-0.3393 (-1.014)	-0.2828 * (-1.868)	-0.0439 (-0.391)	-0.0353 (-0.486)	-0.0560 (-1.262)	-0.0222 (-0.428)	-0.0749 (-1.351)	-0.1056 (-1.471)	-0.2154 ** (-1.990)	-0.5269 ** (-2.810)	-0.7606 * (-1.944)
<i>Transactions</i>	0.4263 ** (3.487)	0.5751 ** (3.199)	0.4955 ** (3.808)	0.4560 ** (3.493)	0.4380 ** (5.229)	0.3764 ** (5.445)	0.4030 ** (5.551)	0.4150 ** (6.163)	0.4439 ** (5.324)	0.5858 ** (5.732)	0.6123 ** (4.432)	0.5348 ** (2.967)
<i>ERC20</i>	-0.0335 * (-1.868)	-0.0638 (-1.197)	-0.0234 (-1.104)	0.0044 (0.316)	-0.0166 ** (-2.241)	-0.0139 ** (-2.980)	-0.0182 ** (-3.006)	-0.0093 (-1.445)	-0.0049 (-0.778)	-0.0090 (-1.006)	-0.0213 (-1.090)	-0.0384 (-1.064)
<i>Block Size</i>	0.3179 ** (2.428)	0.3149 * (1.857)	0.2178 (1.517)	0.1970 (1.627)	0.1218 (1.573)	0.0941 (1.449)	0.0870 (1.402)	0.0634 (1.100)	0.1625 ** (1.986)	0.1966 * (1.790)	0.2212 (1.444)	0.2941 (1.218)
<i>Block Time</i>	0.4785 ** (1.992)	0.4787 (0.749)	0.4115 (0.967)	0.6462 ** (3.279)	0.7725 ** (5.292)	0.6710 ** (4.776)	0.4800 ** (2.875)	0.6679 ** (3.883)	0.5889 ** (2.504)	0.8123 ** (2.969)	0.9136 ** (2.416)	0.8550 (1.210)
<i>Contracts</i>	0.0147 (0.841)	0.0317 (0.619)	0.0331 (1.228)	0.0238 * (1.807)	0.0123 ** (2.017)	0.0092 ** (2.048)	0.0107 ** (2.554)	0.0112 ** (2.386)	0.0116 ** (2.003)	0.0190 * (1.669)	0.0025 (0.086)	-0.0558 (-0.997)

This table reports slope coefficients for each respective quantile  $\theta = \{0.05, 0.10, 0.20, \dots, 0.80, 0.90, 0.95\}$ . The regressors (*Eth Price*, *Transactions*, *ERC20*, *Block Size*, *Block Time*, and *Contracts*, respectively) that are used to explain Ethereum gas price changes are discussed in Section 3 of the article. All data series are transformed into their natural log first-differences (in %) so that they do not contain a unit root in their time series representations (see Table 2). *T*-statistics are in parentheses and estimated using heteroskedasticity-consistent and bootstrapped standard errors. Equations (3) through (9) discuss the bootstrapping quantile regression procedure. Significance at the 5% and 10% levels is indicated by \*\* and \*, respectively. The entire sample period for this analysis is from 1 September 2015 through 26 May 2023 and the frequency of the data is daily (and includes weekend data). OLS estimates are also shown for the sake of comparison. The constant is included in the estimations of the quantile regression and OLS, respectively, but is not reported here for brevity. *T*-statistics for the OLS estimation is performed using heteroskedasticity and autocorrelation-consistent Newey–West standard errors.

From the OLS and quantile regression estimates, respectively, the following broad findings emerge. First, and with the exception of changes in the number of intraday transactions on the Ethereum blockchain (*Transactions*), the predictor variables are not necessarily significant across all conditional quantiles. Thus, their explanatory power can differ with respect to days of high versus low gas price volatility, of either sign. For example, the coefficient estimates for changes in the intraday number of Ethereum requests for comment (*ERC20*) are significant at the 5% level only in the 30th, 40th, and 50th conditional quantiles, respectively. Likewise, the coefficient estimates for changes in the intraday number of total verified smart contracts (*Contracts*) are significant at the 5% level only in the 30th, 40th, 50th, 60th, and 70th conditional quantiles, respectively.

Second, while the signs of several of the coefficients are consistent with a priori expectations, others are not as straightforward to explain. For example, as *Transactions* rise across time, this is associated with a positive change in Ethereum gas prices—a relation that holds steady during periods of both high and low gas price volatility. Such a finding is to be expected, since rising demand for validators on the Ethereum blockchain is likely to be associated with rising transaction costs. As shown in Equations (1) and (2), rising

demand (congestion) in the Ethereum blockchain will lead to rises in the future base fee. Likewise, we see that the sign for the coefficient *Block Time* is also positive and significant at the 5% level for all conditional quantiles, with the exception of those which correspond with extreme gas price volatility (specifically, when  $\theta = 0.05, 0.10,$  and  $0.95,$  respectively). This is consistent with the technological and economic underpinnings of EIP-1559, which seeks to '(self-)regulate' the degree of congestion within the Ethereum ecosystem.

Third, another major observation from the results in Table 3 is that while some OLS regression estimates are statistically significant, this is likely driven by a certain cross-section of the empirical distribution of gas price changes. For example, when we look at the coefficient *Block Size*, we see that it is positive and significant at the 5% level when estimated using OLS. When viewing its statistical significance across quantiles, however, we see that it is significant only in the 70th and 80th conditional quantiles at the 5% and 10% levels, respectively. While block sizes in the Ethereum ecosystem vary across time, there is a growing body of research that examines whether there exist optimal limits in the size of blocks for Ethereum or other cryptocurrencies (Leal et al. 2020).

Finally, the remaining predictor variables (*Eth Price*, *ERC20*, and *Contracts*) either yield mixed results or bear signs that are opposite to what we would expect to see. For example, and from the OLS results, *Eth Price* has a negative sign. This suggests that, on average, rises in the price for Ethereum are associated with declining gas prices. While investors who actively trade Ethereum on the various cryptocurrency exchanges may not be directly or simultaneously involved in using its blockchain to transfer Ether or execute smart contracts, it is not unreasonable to expect that rising prices are associated with rising overall user and investor sentiment (Sockin and Xiong 2023). It will be worthwhile to examine this finding in future research, especially since Pierro and Rocha (2019) show that it is unlikely that the market price of Ethereum can lead to changes in Ethereum gas prices. Moreover, *ERC20* and *Contracts* are not significant in OLS representations at the 5% level of significance. In particular, and while *Contracts* bears a positive sign consistent with our a priori expectations, significance is shown in the center of the distribution (when  $\theta = 0.30, 0.40, 0.50, 0.60,$  and  $0.70,$  respectively). As shown in Panel B of Table 1, however, and given the nature of the data series, *Contracts* exhibits some of the largest values in the tails of its distribution when compared to the other variables. Given the large degree of tail uncertainty it exhibits, this is the likely reason for its statistical insignificance in the OLS representation.

## 6. Summary and Future Research

This article explores the network determinants of Ethereum transaction fees. Such fees are referred to as "gas prices" in the Ethereum blockchain. Unlike the transaction fees found in other blockchain-based cryptocurrencies, gas prices embody distinguishing properties and mechanics given that the Ethereum network supports decentralized applications (dApps) and smart contracts.

Drawing on some of the key Ethereum network activity variables, this article analyzes and identifies the determinants of Ethereum gas prices. Using a bootstrapped quantile regression model, it can be seen that network activity, such as the sizes of blocks or the number of transactions and contracts, can show a heterogeneous relationship with gas prices across periods of low and high gas price changes. The quantile regression method demonstrates that linear modeling techniques may only yield a partial view of the rich dynamics found in the full range of gas prices' conditional distribution. More broadly, this article shows the challenges in modeling and explaining the determinants of gas prices. Its findings echo the warnings of Buchinsky (1998), who argued that "...potentially different solutions at distinct quantiles may be interpreted as differences in the response of the dependent variable to changes in the regressors at various points in the conditional distribution of the dependent variable. ...".

These findings are thus of interest, especially in light of the recent implementation of the Ethereum Improvement Proposal (EIP) 1559, which aims, in part, to provide an

algorithmic updating rule to estimate Ethereum’s “base fee”—the minimum amount of “gas” required for a transaction to be completed and included into a block.

Future research can continue to develop theoretical frameworks and modeling techniques that, first, identify the microstructure determinants of Ethereum gas prices and, second, model their interactions with gas prices across critical technological and economic regimes. As mentioned, one of the motivations for the bootstrapped quantile regression approach in this article was the implementation of EIP-1559 and when Ethereum moved fully to PoS from PoW. These points in its history represent critical regime changes that are not only technological but economic in nature, given that they can change the way validators or investors behave.

Linear regression models are unlikely to uncover the rich dynamics and interactions that can exist among variables in the presence of such fundamental regime shifts. Thus, future research questions such as *are periods with surging gas prices linked to particular states of Ethereum’s microstructure versus periods with declining gas prices? Is the probability of rising (declining) gas prices time-varying in nature? Is it possible that the microstructures of other cryptocurrencies have any impact on Ethereum’s microstructure or its gas prices?* Answers to questions such as these can have important implications across a wide range of disciplines in not only financial economics, but in computer science and technology, operations research, and behavioral psychology. This is especially true since Ethereum’s diverse ecosystem involves human users that interact with autonomous agents (such as smart contracts).

As future research considers these questions, it is crucial to reiterate the importance of understanding technological and economic regime shifts in cryptocurrencies and their markets, and utilizing methodological frameworks that can account for this. The bootstrapped quantile regression approach here is but one approach. Li and Wang (2017), who examine the behavior of bitcoin prices, conclude as follows: “. . .while it is valuable at this stage to establish a research framework and test its utility. . .the relationships we identified could be subject to further changes as exchange markets develop. . .it will be necessary to revisit the model at some future time and consider the possibility of multiple regime changes in exchange rate dynamics. . .” (p. 59).

**Funding:** This research received no external funding.

**Data Availability Statement:** The data examined in this study are openly available through Ethereum’s blockchain, as well as through online resources and APIs (these are discussed in note (1) of the study).

**Conflicts of Interest:** The author declares no conflict of interest.

## Notes

- <sup>1</sup> Consistent with the open, decentralized, and transparent philosophy of blockchain technology, there is a plethora of publicly available online resources and APIs for extracting and analyzing Ethereum gas prices and network data. Some of the data resources used in this article, as well as informational sources, are as follows: QuickNode ([www.quicknode.com](http://www.quicknode.com), accessed on 20 August 2023), Etherscan ([etherscan.io](https://etherscan.io)), Ethereum.org (<https://ethereum.org/en/developers/docs/gas/>, accessed on 20 August 2023), and Blocknative (<https://www.blocknative.com/gas-platform>, accessed on 20 August 2023), to name a few.
- <sup>2</sup> See, for example, <https://etherscan.io/contractsVerified>, accessed on 20 August 2023.

## References

- Azouvi, Sarah, Guy Goren, Alexander Hicks, and Lioba Heimbach. 2023. Base fee manipulation in Ethereum’s EIP-1559 transaction fee mechanism. *arXiv* arXiv:2304.11478.
- Bowden, James, Timothy King, Dimitrios Koutmos, Tiago Loncan, and Francesco Saverio Stentella Lopes. 2021. A taxonomy of fintech innovation. In *Disruptive Technology in Banking and Finance: An International Perspective on FinTech*. Cham: Palgrave Macmillan, pp. 47–91.
- Buchinsky, Moshe. 1994. Changes in the US wage structure 1963–1987: Application of quantile regression. *Econometrica* 62: 405–58. [\[CrossRef\]](#)
- Buchinsky, Moshe. 1995. Estimating the asymptotic covariance matrix for quantile regression models: A Monte Carlo study. *Journal of Econometrics* 68: 303–38. [\[CrossRef\]](#)
- Buchinsky, Moshe. 1998. Recent advances in quantile regression models: A practical guideline for empirical research. *Journal of Human Resources* 33: 88–126. [\[CrossRef\]](#)

- Buterin, Vitalik. 2014. A Next-Generation Smart Contract and Decentralized Application Platform. Ethereum White Paper. Available online: [https://www.the-blockchain.com/docs/Ethereum\\_white\\_paper-a\\_next\\_generation\\_smart\\_contract\\_and\\_decentralized\\_application\\_platform-vitalik-buterin.pdf](https://www.the-blockchain.com/docs/Ethereum_white_paper-a_next_generation_smart_contract_and_decentralized_application_platform-vitalik-buterin.pdf) (accessed on 20 August 2023).
- Cai, Cynthia Weiyi. 2018. Disruption of financial intermediation by FinTech: A review on crowdfunding and blockchain. *Accounting & Finance* 58: 965–92.
- Dannen, Chris. 2017. *Introducing Ethereum and Solidity: Foundations of Cryptocurrency and Blockchain Programming for Beginners*. Berkeley: Apress.
- Dickey, David A., and Wayne A. Fuller. 1981. Likelihood ratio statistics for autoregressive time series with a unit root. *Econometrica* 49: 1057–72. [CrossRef]
- Dylag, Matthew, and Harrison Smith. 2023. From cryptocurrencies to cryptocourts: Blockchain and the financialization of dispute resolution platforms. *Information, Communication & Society* 26: 372–87.
- Faqir-Rhazoui, Youssef, Miller-Janny Ariza-Garzón, Javier Arroyo, and Samer Hassan. 2021. Effect of the gas price surges on user activity in the DAOs of the Ethereum Blockchain. Paper presented at Extended Abstracts of the 2021 CHI Conference on Human Factors in Computing Systems, Yokohama, Japan, May 8–13; pp. 1–7.
- Fernandez-Carames, Tiago M., and Paula Fraga-Lamas. 2020. Towards post-quantum blockchain: A review on blockchain cryptography resistant to quantum computing attacks. *IEEE Access* 8: 21091–116. [CrossRef]
- Gligor, David Marius, Beth Davis-Sramek, Albert Tan, Alex Vitale, Ivan Russo, Ismail Golgeci, and Xiang Wan. 2022. Utilizing blockchain technology for supply chain transparency: A resource orchestration perspective. *Journal of Business Logistics* 43: 140–59. [CrossRef]
- Hölbl, Marko, Marko Kompara, Aida Kamišalić, and Lili Nemec Zlatolas. 2018. A systematic review of the use of blockchain in healthcare. *Symmetry* 10: 470. [CrossRef]
- Huber, Peter. 1967. The behavior of maximum likelihood estimates under nonstandard conditions. In *Proceedings of the Fifth Berkeley Symposium on Mathematical Statistics and Probability*. Berkeley: The Regents of the University of California, vol. 1, pp. 221–33.
- King, Timothy, Dimitrios Koutmos, and Francesco Saverio Stentella Lopes. 2021. Cryptocurrency mining protocols: A regulatory and technological overview. In *Disruptive Technology in Banking and Finance: An International Perspective on FinTech*. Cham: Palgrave Macmillan, pp. 93–134.
- Koenker, Roger, and Gilbert Bassett Jr. 1978. Regression quantiles. *Econometrica* 46: 33–50. [CrossRef]
- Koutmos, Dimitrios, and Wang Chun Wei. 2023. Nowcasting bitcoin's crash risk with order imbalance. *Review of Quantitative Finance and Accounting* 61: 125–54. [CrossRef]
- Kshetri, Nir, and Jeffrey Voas. 2018. Blockchain-enabled e-voting. *IEEE Software* 35: 95–99. [CrossRef]
- Kwiatkowski, Denis, Peter CB Phillips, Peter Schmidt, and Yongcheol Shin. 1992. Testing the null hypothesis of stationarity against the alternative of a unit root: How sure are we that economic time series have a unit root? *Journal of Econometrics* 54: 159–78. [CrossRef]
- Leal, Fátima, Adriana E. Chis, and Horacio González-Vélez. 2020. Performance evaluation of private ethereum networks. *SN Computer Science* 1: 285. [CrossRef]
- Leonardos, Stefanos, Barnabé Monnot, Daniël Reijtsbergen, Efstratios Skoulakis, and Georgios Piliouras. 2021. Dynamical analysis of the EIP-1559 Ethereum fee market. Paper presented at the 3rd ACM Conference on Advances in Financial Technologies, Arlington, VA, USA, September 26–28; pp. 114–26.
- Li, Xin, and Chong Alex Wang. 2017. The technology and economic determinants of cryptocurrency exchange rates: The case of Bitcoin. *Decision Support Systems* 95: 49–60. [CrossRef]
- Lipton, Alexander. 2018. Blockchains and distributed ledgers in retrospective and perspective. *Journal of Risk Finance* 19: 4–25. [CrossRef]
- Liu, Yulin, Yuxuan Lu, Kartik Nayak, Fan Zhang, Luyao Zhang, and Yinhong Zhao. 2022. Empirical analysis of eip-1559: Transaction fees, waiting times, and consensus security. Paper presented at the 2022 ACM SIGSAC Conference on Computer and Communications Security, Copenhagen, Denmark, November 26–30; pp. 2099–113.
- Marzo, Giordano De, Francesco Pandolfelli, and Vito D. P. Servedio. 2022. Modeling innovation in the cryptocurrency ecosystem. *Scientific Reports* 12: 12942. [CrossRef]
- Nakamoto, Satoshi. 2008. Bitcoin: A Peer-to-Peer Electronic Cash System. Available online: <https://bitcoin.org/bitcoin.pdf> (accessed on 20 August 2023).
- Ochôa, Iago Sestrem, Valderi Reis Quietinho Leithardt, Leonardo Calbusch, Juan Francisco De Paz Santana, Wemerson Delcio Parreira, Laio Oriel Seman, and Cesar Albenes Zeferino. 2021. Performance and security evaluation on a blockchain architecture for license plate recognition systems. *Applied Sciences* 11: 1255. [CrossRef]
- Oliva, Gustavo A., Ahmed E. Hassan, and Zhen Ming Jiang. 2020. An exploratory study of smart contracts in the Ethereum blockchain platform. *Empirical Software Engineering* 25: 1864–904. [CrossRef]
- Pedersen, Thomas Q. 2015. Predictable return distributions. *Journal of Forecasting* 34: 114–32. [CrossRef]
- Phillips, Peter C. B., and Pierre Perron. 1988. Testing for a unit root in time series regression. *Biometrika* 75: 335–46. [CrossRef]
- Pierro, Giuseppe Antonio, and Henrique Rocha. 2019. The influence factors on Ethereum transaction fees. Paper presented at 2019 IEEE/ACM 2nd International Workshop on Emerging Trends in Software Engineering for Blockchain (WETSEB), Montreal, QC, Canada, May 27; pp. 24–31.

- Powell, James L. 1986. Censored regression quantiles. *Journal of Econometrics* 32: 143–55. [\[CrossRef\]](#)
- Rahimian, Reza, Shayan Eskandari, and Jeremy Clark. 2019. Resolving the multiple withdrawal attack on ERC20 tokens. Paper presented at 2019 IEEE European Symposium on Security and Privacy Workshops (EuroS&PW), Stockholm, Sweden, June 17–19; pp. 320–29.
- Reijsbergen, Daniël, Shyam Sridhar, Barnabé Monnot, Stefanos Leonardos, Stratis Skoulakis, and Georgios Piliouras. 2021. Transaction fees on a honeymoon: Ethereum’s EIP-1559 one month later. Paper presented at 2021 IEEE International Conference on Blockchain (Blockchain), Melbourne, Australia, December 6–8; pp. 196–204.
- Risius, Marten, Christoph F. Breidbach, Mathieu Chanson, Ruben von Krannichfeldt, and Felix Wortmann. 2023. On the performance of blockchain-based token offerings. *Electronic Markets* 33: 32. [\[CrossRef\]](#)
- Saberi, Sara, Mahtab Kouhizadeh, Joseph Sarkis, and Lejia Shen. 2019. Blockchain technology and its relationships to sustainable supply chain management. *International Journal of Production Research* 57: 2117–35. [\[CrossRef\]](#)
- Sockin, Michael, and Wei Xiong. 2023. A model of cryptocurrencies. *Management Science*, forthcoming. [\[CrossRef\]](#)
- Vacca, Anna, Andrea Di Sorbo, Corrado A. Visaggio, and Gerardo Canfora. 2021. A systematic literature review of blockchain and smart contract development: Techniques, tools, and open challenges. *Journal of Systems and Software* 174: 110891. [\[CrossRef\]](#)
- Walker, Donald A. 1988. Iteration in Walras’s theory of tatonnement. *De Economist* 136: 299–316. [\[CrossRef\]](#)
- Wheatley, Spencer, Didier Sornette, Tobias Huber, Max Reppen, and Robert N. Gantner. 2019. Are Bitcoin bubbles predictable? Combining a generalized Metcalfe’s law and the log-periodic power law singularity model. *Royal Society Open Science* 6: 180538. [\[CrossRef\]](#)
- Yuan, Yong, and Fei-Yue Wang. 2018. Blockchain and cryptocurrencies: Model, techniques, and applications. *IEEE Transactions on Systems, Man, and Cybernetics: Systems* 48: 1421–28. [\[CrossRef\]](#)
- Zheng, Peilin, Zigui Jiang, Jiajing Wu, and Zibin Zheng. 2023. Blockchain-based decentralized application: A survey. *IEEE Open Journal of the Computer Society* 4: 121–33. [\[CrossRef\]](#)

**Disclaimer/Publisher’s Note:** The statements, opinions and data contained in all publications are solely those of the individual author(s) and contributor(s) and not of MDPI and/or the editor(s). MDPI and/or the editor(s) disclaim responsibility for any injury to people or property resulting from any ideas, methods, instructions or products referred to in the content.